CHARACTERIZATION OF MULTILAYER LUMINESCENT SOLAR CONCENTRATORS

A. Bozzola[1], S. Flores Daorta[1], M. Galli[1], M. Patrini[1], L.C. Andreani[1],
A. Alessi[2], R. Fusco[2], A. Proto[2], P. Scudo[2]
[1] *Dipartimento di Fisica "A. Volta" and UdR CNISM, Università degli Studi di Pavia, Italy*
[2] *ENI S.p.a. Research Center for Non-Conventional Energies – Istituto ENI Donegani, Novara, Italy*

ABSTRACT: We present an experimental study of multilayer luminescent solar concentrators (LSCs) based on spectroscopic characterization and external quantum efficiency measurement, which is assumed as figure of merit for this work. We focus on two types of LSCs: polymeric and liquid-based. Our aim is to study the photovoltaic conversion of solar energy by means of solar spectrum splitting by the LSC, to evaluate the effects of dyes' concentrations on absorption of sunlight and on self-absorption of emitted fluorescence, and finally to evaluate the effects of LSCs' sizes on their performance. Single-layer and bi-layer LSCs are considered, based on one or more types of fluorescent dyes.

Keywords: Concentrators, photoluminescence, spectral response.

1 INTRODUCTION

Luminescent solar concentrators (LSCs) are hybrid photovoltaic devices in which sunlight in absorbed by organic or inorganic fluorophores (dyes) dispersed in a solid or liquid matrix (Fig. 1). Emitted fluorescence is guided within the matrix bulk by total internal reflections until it reaches its edges, where photovoltaic (PV) cells are applied [1-5].
In principle, LSCs have many advantages over conventional PV cells. Since the edge area of PV cells is much smaller than the LSC's surface area, the amount of required semiconductor material is far reduced, leading to a reduction of the total device costs. Furthermore, since absorption of sunlight and fluorescence emission are distinct process (the latter being governed only by total internal reflection inside the LSC), these devices can act as concentrators for both direct and diffuse sunlight without requiring any auxiliary tracking systems. This feature allows to reduce the device costs with respect to common concentrator systems which make use of mirrors or lenses to track the sun in its apparent motion so to harvest only direct sunlight. Finally, LSCs can be made semi-transparent by a proper choice of dyes absorbing only in the ultraviolet (UV) and high-energy visible (VIS) spectral ranges, and this feature is desirable for applications in windows, greenhouses and other building-integrated photovoltaic structures.
In this work we propose an experimental characterization of LSCs by means of external quantum efficiency (EQE) measurements. From the EQE, short-circuit current density J_{sc} can be derived according to the formula

$$J_{sc} = -e \int_0^{+\infty} EQE(\lambda) b_s(\lambda) d\lambda \,, \qquad (1)$$

where b_s is the incident AM 1.5 solar photon flux, reported in Fig. 2(a) in arbitrary units (for quantitative data see, for example, [6]).
In our work special attention is paid to the following characterizing features of LSCs: (i) effects of dye absorption in different spectral ranges of the solar spectrum; (ii) effects dye concentrations on absorption of incident sunlight and self-absorption of emitted fluorescence; (iii) effects of LSCs' size on the performance of final devices.

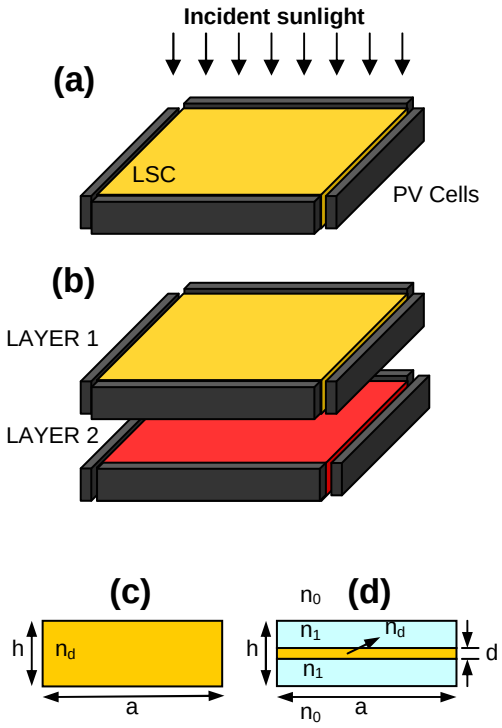

Figure 1: Schematic representations of a single-layer LSC coupled with silicon PV cells at the edges **(a)**, and of a bi-layer LSC **(b)**. LSC configurations under exam: polymeric **(c)**, and liquid-based LSC **(d)**.

2 DEVICES UNDER INVESTIGATION

LSCs under investigation are represented in Fig. 1. We study both single-layer and bi-layer LSCs, which are shown, respectively, in Figs. 1(a) and 1(b). Single-layer LSCs can be doped with one or more types of fluorescent dyes, and are particularly suited for the production of semi-transparent devices. In our work we consider three types of organic fluorescent dyes, briefly denoted as A, B and C [7]. Absorption is described in terms of the molar extinction coefficient ε which has dimensions of [$cm^{-1}M^{-1}$] (where M is the molar concentration of the dye in the matrix material), while emitted fluorescence is described in terms of the normalized emission spectrum $\overline{b_e}$,

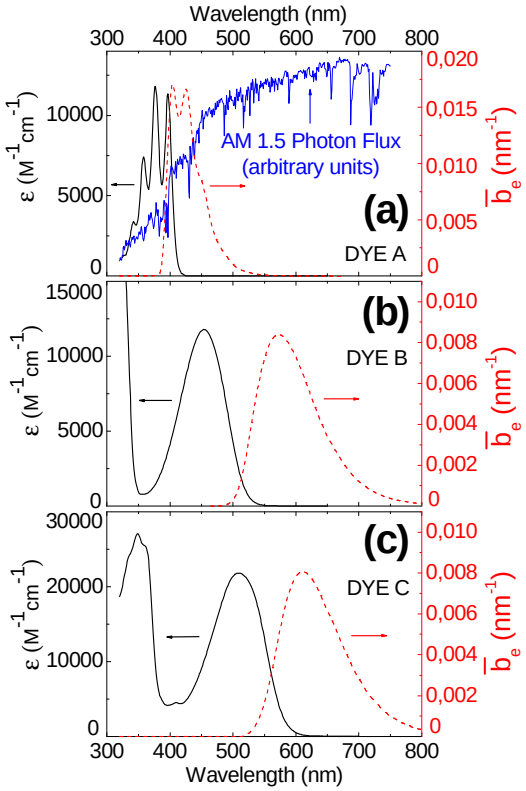

Figure 2: Molar extinction coefficients ε (black solid lines) and normalized emission spectra $\bar{b}_e$ (red dashed lines) for dye A (**a**), dye B (**b**) and dye C (**c**).

which satisfies the condition:

$$\int_0^{+\infty} \bar{b}_e(\lambda)d\lambda = 1 \qquad (2)$$

Optical spectra of molar extinction coefficients ε and normalized emission $\bar{b}_e$ are shown in Figs. 2(a), 2(b) and 2(c) for dyes A, B and C respectively. For single-layer LSCs we considered the cases of a combination of dyes A and B, dye B alone or dye C alone.

Bi-layer LSCs are shown in Fig. 1(b). In this case the top layer is doped with a combination of dyes A and B or dye B alone, while the bottom layer is doped with dye C alone.

In terms of layer's structure, two configurations have been tested, namely polymeric LSCs and liquid-based LSCs, which are shown in Figs. 1(c) and 1(d) respectively. Polymeric LSCs are made of square slabs of poly methyl - methacrylate (PMMA) in which fluorescent dyes are dispersed. The refractive index n_d of PMMA is equal to 1.5, which gives a reflectance R~0.04 at the interface between PMMA and air. The thickness h of the PMMA slabs is 0.65 cm, and it is equal to the width of the PV cells applied at the edges. The side length of the slabs is denoted with a, and it is equal to a multiple of the length of the applied PV cells (2.2 cm). For the case of polymeric LSCs, all four lateral edges are covered with PV cells, but, in order to reduce the number of PV cells, some lateral edges can be covered with mirrors as well.

Liquid-based LSCs are shown in Fig. 1(d) and are obtained by filling a squared quartz couvette of refractive index n_1~1.45 with a solution of 1,2-dichlorobenzene (the solvent, whose refractive index n_d is equal to 1.55) and fluorescent dye. The thickness h of the couvette is the same of polymeric slabs, while the internal width d is equal to 0.1 cm. This implies that the concentrations of fluorescent dyes have to be 6.5 times higher in the couvette with respect to PMMA slabs in order to reach the same degree of absorption.

For both polymeric and liquid-based LSCs, lateral PV cells are kept in optical contact with the edges of the LSCs by means of a transparent index-matching gel, which prevents strong reflection losses at the interface.

3 EXTERNAL QUANTUM EFFICIENCY FOR THE DEVICES

3.1 Theoretical Model

In order to derive an expression for the EQE of LSC devices, it is convenient to decompose their global working mechanism into three steps and to analyze them separately, assuming that only one kind of fluorescent dye is dispersed in the LSC. The global working mechanism can be decomposed into:

- Absorption of sunlight by fluorescent dyes;
- Emission and propagation of fluorescence through the LSC;
- Photovoltaic conversion of fluorescence at the edges of the LSC.

Absorption of sunlight is the first working step and the main physical quantities involved are reflectance R of the interface between LSC and air, molar extinction coefficient ε and molar concentration C of the dispersed dye. The absorption probability for incident photons at wavelength λ can thus be expressed as

$$P_{abs}(\lambda) = [1 - R(\lambda)][1 - e^{-\ln(10)C\varepsilon(\lambda)h}] \qquad (3)$$

Emission of fluorescence is determined by the quantum yield QY of the dye, by its emission pattern (which has spherical symmetry for the dyes under examination [7]) and by the normalized emission spectrum $\bar{b}_e$.

Propagation of fluorescence through the LSC, instead, is described by the fraction f of fluorescence that can reach the edges by total internal reflection and by the collection probability P_c. For the case of polymeric LSCs with all four edges covered by PV cells, the fraction f is equal to 0.74, and it is determined only by the refractive indeces of the matrix material and air. The collection probability P_c is determined by self-absorption of the emitted fluorescence, by absorption of the matrix material, and by the losses deriving from scattering inside the LSC and at the surface (where a fraction of fluorescence can escape). In an ideal LSC, P_c is taken equal to unity, but in a real device it is always less than unity. Furthermore, the greater the LSC, the smaller the collection probability will be, since losses become more relevant for longer propagation distances (in this context we refer to it as *size effects*). From the above considerations it follows that emitted photons at wavelength λ' can reach the edges of the LSC with a probability P_g given by

$$P_g(\lambda') = QY \cdot f \cdot P_c(\lambda') \cdot \bar{b}_e(\lambda')d\lambda' \qquad (4)$$

Photovoltaic conversion of the fluorescence that reaches the edges of the LSC is determined by the external

quantum efficiency EQE_{PV} of the applied PV cells, neglecting reflection losses at the interfaces between LSC and PV cells. From the above considerations, it follows that the global external quantum efficiency EQE_{L1} for a single-layer LSC device (Fig 1(a)) with a single fluorescent dye can be expressed as

$$EQE_{L1}(\lambda) = P_{abs}(\lambda) \int_{\lambda'>\lambda} P_g(\lambda')EQE_{PV}(\lambda') = [1-R(\lambda)][1-e^{-\ln(10)C\varepsilon(\lambda)h}] \int_{\lambda'>\lambda} [QY \cdot f \cdot P_c(\lambda') \cdot \bar{b}_e(\lambda')]EQE_{PV}(\lambda')d\lambda' \quad (5)$$

When two or more types of fluorescent dyes are dispersed in the same slab (for example, in our case, dye A and dye B), some changes have to be applied in Eq. (5) to take into account cross-absorption, namely the fact that a relevant fraction of fluorescence photons emitted by dye A can be re-absorbed by dye B before reaching the lateral PV cells. Cross absorption as well as self-absorption are rather difficult to evaluate analytically. A possible solution is to evaluate them numerically, using, for example, a Monte Carlo approach [8].
For a bi-layer LSC device (Fig. 1(b), where both layers are assumed to be doped with a single dye) different expressions can be derived for the EQE of the two layers. For the top layer, Eq. (5) is valid. For the bottom layer, Eq. (5) has to be multiplied by a factor $[1-R]^2[e^{-\ln(10)C\varepsilon h}]_{L1}$ which takes into account that photons reflected or absorbed in the top layer cannot contribute to the EQE of the bottom layer.

3.2 Experimental setup for EQE measurement

The experimental setup used for the optical characterization of LSC devices is shown in Fig. 3. The external quantum efficiency EQE_{LSC} of the studied devices is obtained comparing the short-circuit current developed by the devices with that of a calibrated, reference c-Si PV cell (whose external quantum efficiency is denoted as EQE_{ref}) under illumination with monochromatic light. A halogen lamp is used as light source, and a monochromator is used to produce the monochromatic beam at a given wavelength λ. Before entering the monochromator, light is focused on the entrance slits by means of a pair of fused silica lenses (L in Fig. 3) and modulated with an optical chopper, which is phase-matched with a lock-in amplifier. We use modulated light and lock-in amplifier in order to minimize effects produced by external light, which causes spurious DC current contributions when devices are in short-circuit conditions. Monochromatic light escaping the monochromator is sent onto a beam splitter (BS in Fig. 3), whose reflectance R_{BS} and transmittance T_{BS} are known. Reflected light is then focused on the reference cell, while transmitted light is directed onto the device under investigation, providing its uniform illumination and preventing direct illumination of the lateral PV cells. Short-circuit currents (which contain both DC and AC contributions) developed by the reference cell and by the device are converted to voltage signals $V_{ref}(\lambda)$ and $V_{LSC}(\lambda)$ and pre-amplified with gains equal to G_{ref} and G_{LSC} respectively. Then signals are sent to the lock-in amplifier, which selects only the AC components that contain the physical signals of interest. With a simultaneous measurement of the voltages $V_{ref}(\lambda)$ and $V_{LSC}(\lambda)$, one can obtain the external quantum efficiency $EQE_{LSC}(\lambda)$ of the device under investigation as

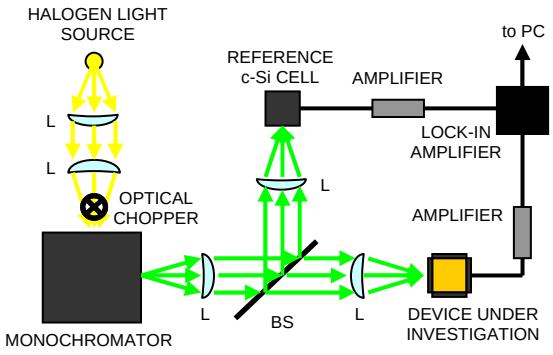

Figure 3: Scheme of the experimental setup used for external quantum efficiency measurement.

$$EQE_{LSC}(\lambda) = \frac{R_{BS}G_{ref}}{T_{BS}G_{LSC}} \frac{I_{LSC}(\lambda)}{I_{ref}(\lambda)} EQE_{ref}(\lambda) \quad (6)$$

The spectral range available for EQE measurement is 350-1100 nm and it is determined by the range of calibration values of the reference c-Si cell.

4 RESULTS

4.1 External quantum efficiency for single-layer LSCs

We study single-layer LSCs doped with one type of fluorescent dye (B or C) or with two types of dyes (A and B). Results of EQE measurements for liquid-based LSCs doped with dye B and C are shown in Figs. 4(a) and 4(b) respectively, for different concentrations C of the dyes. Both device responses have common features. For low concentrations, the EQE is mostly determined by the molar extinction coefficient ε, with a peak at the absorption maximum (at λ=450 nm for dye B, and at λ=510 nm for dye C). Increasing the concentration, the absorption saturates and the EQE reaches a plateau. Actually, as it is evident from the data, the EQE is not perfectly constant, and this is due to self-absorption of the emitted fluorescence. To understand this last point, one has to take into account that fluorescence is emitted at lower energy than the excitation energy, or, in other words, the fluorescence wavelength λ' is larger than excitation wavelength λ. When one excite the LSC with a short wavelength λ, fluorescence photons are emitted over the whole emission spectrum $\bar{b}_e$, and the overlap between $\bar{b}_e$ and ε determines self-absorption. On the other hand, for longer excitation wavelengths λ, fluoresced photons will be emitted at longer wavelengths λ', and a smaller fraction of them will be emitted in the

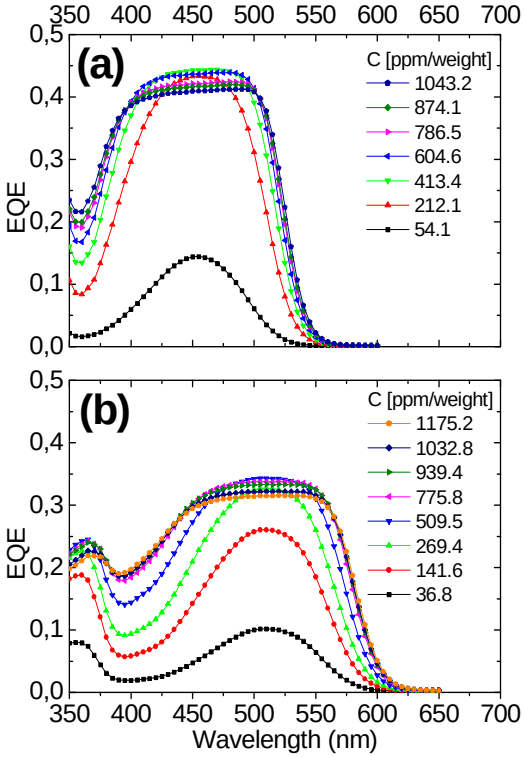

Figure 4: (**a**) External quantum efficiency for dye B and (**b**) for dye C in 1,2-dichlorobenzene in liquid-based LSCs for different concentrations of the dyes.

overlap region between ε and $\bar{b}_e$, thus reducing self-absorption and giving an higher EQE. Optimal concentrations C for dyes are those which produce the maximum short-circuit current densities J_{sc}, and they depend on the size of the LSC, giving higher C for smaller devices, and lower C for bigger ones, since self-absorption losses are more relevant in the latter case.

When concentrations are increased above the optimal one, the EQE spectrum becomes slightly broader, but the central plateau starts decreasing due to increased self-absorption losses which are not compensated by further gains, since absorption is already saturated.

Results on liquid-based single-layer LSCs are summarized in Fig. 5. EQEs at optimal concentrations are reported in Fig. 5(a) for LSCs doped with dye A and dye B (blue line), dye B alone (black line) and dye C alone (red line). As evident, when dye A is added to dye B in a liquid LSC, the EQE is increased in the UV spectral range. However, since the solar photon flux is rather poor at high energy, only a very small increase in short-circuit current density is produced with respect to dye B alone. The EQE for LSCs with dye C alone is lower than that of dye B, and this is due to the fact that fluorescence quantum yield QY for dye C in 1,2-dichlorobenzene is just 0.7, compared with 0.95 of dye A and B in the same solvent [7]. Starting from the data of Figs. 4(a) and 4(b), short-circuit current densities J_{sc} have been calculated according to Eq. (1) and are reported in Fig. 5(b) for different concentrations of dye B and dye C. As it is evident, in spite of its lower QY, dye C develops higher J_{sc} than dye B, and this is due to the fact that the solar photon flux is richer in the absorbing range of dye C than in that of dye B.

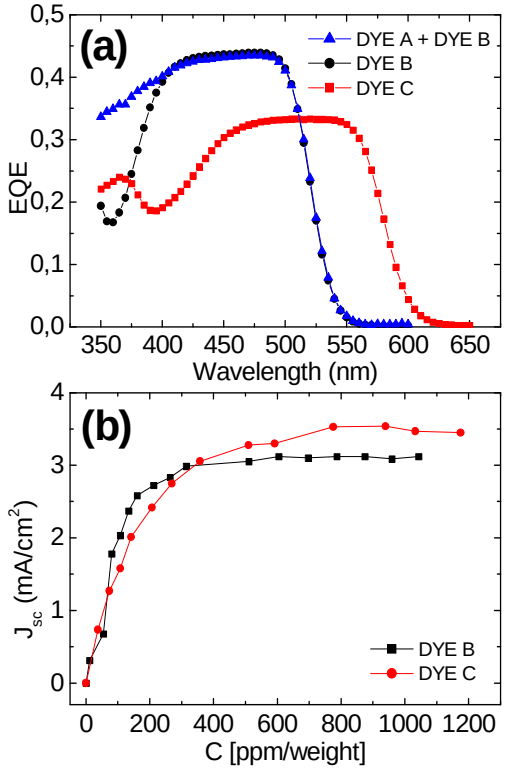

Figure 5: (**a**) External quantum efficiency for liquid-based, single-layer LSC with dye A and dye B (blue line), dye B (black line) and dye C only (red line) at optimal concentrations. (**b**) Short-circuit current density J_{sc} developed by single-layer LSC as a function of dye's concentration.

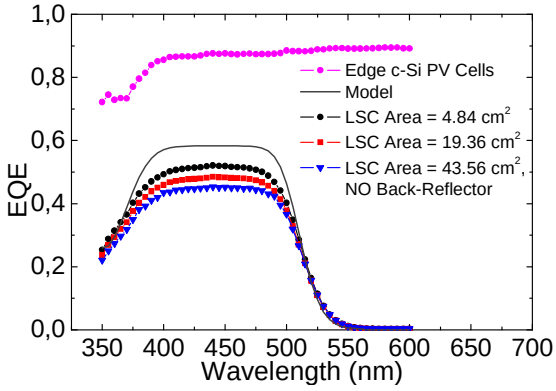

Figure 6: External quantum efficiency for polymeric LSCs with dye A and dye B at optimal concentrations for different LSC sizes.

Results of EQE measurements for polymeric LSCs of different sizes doped with dye A and dye B are shown in Fig. 6, together with the measured EQE_{PV} of the applied lateral c-Si PV cells (top line). As evident from the data, the EQE decreases for bigger devices, since propagation losses become more relevant. Furthermore, for the case of polymeric LSCs, dye A does not produce any particular effect in the EQE, differently from the case of liquid-based LSCs, as it is evident comparing Fig. 5(a) and Fig. 6.

For comparison, also the EQE calculated with Eq. (5) for LSCs with dye B only and without any loss is reported

with a solid grey line: the model can fit quite well experimental data at high energy, even if it does not take into account dye A. A possible explanation of this behavior is that the polymeric matrix material (PMMA) is not completely transparent in the UV spectral range, differently from the case of fused silica and 1,2-dichlorobenzene, which are transparent for wavelengths above 320 nm. This causes incident light to be absorbed by PMMA rather than by dye A, giving lower EQE for the devices in the UV spectral range

4.2 External quantum efficiency for bi-layered LSCs

We study liquid-based bi-layered LSCs in which the top layer (layer 1) is doped with dye A and dye B at optimal concentrations, while the bottom layer (layer 2) is doped with dye C. Results of EQE measurements are shown in Fig. 7(a): the EQE of layer 1 is plotted in black, and it is the same of Fig. 5(a) (blue line), while the EQE of layer 2 is measured for different concentrations of dye C. As evident from the data, the peak of the EQE is lower than that of the top layer, due to the lower *QY* of dye C. Furthermore, the whole EQE spectrum is narrower in the case of dye C in layer 2, since most of the incident light at wavelengths λ below 525 nm is absorbed within the top layer and does not contribute to the EQE of the bottom layer. From *EQE* measurements, the short-circuit current density J_{sc} is calculated according to Eq. (1) for different concentrations of dye B and dye C, and results are shown in Fig. 7(b). The J_{sc} developed by layer 1 is the same of Fig. 5(b) and it is represented with a black line. The J_{sc} for the bottom layer is represented by a red line, and is found to be less than one half of the J_{sc} of layer 1 due to a partial overlap of the absorption spectra of dyes B and C.

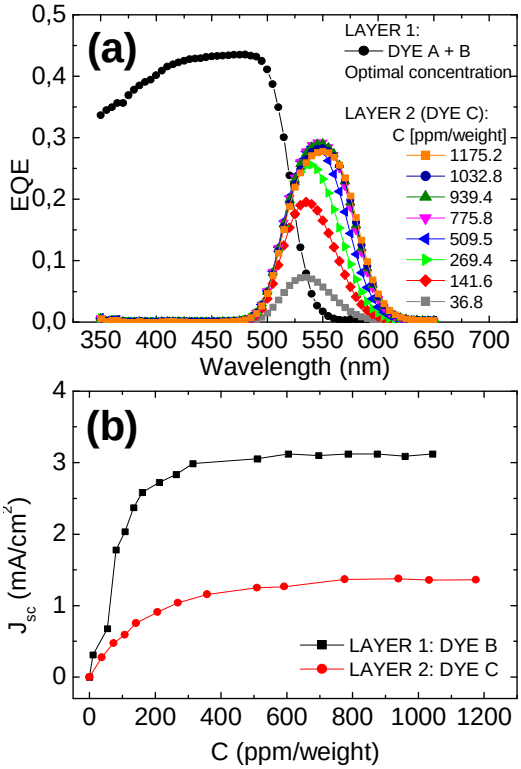

Figure 7: (**a**) External quantum efficiency for 2-layers LSC with dye A and dye B at optimal concentrations in the first layer (black line), and dye C in the second layer (red line) for different concentrations of dye C. (**b**) Short-circuit current density J_{sc} developed by 2-layers LSC as a function of dyes' concentration.

5 CONCLUSIONS

Photovoltaic devices made of single-layer and bi-layer LSCs coupled to c-Si solar cells have been investigated and characterized by means of external quantum efficiency (EQE) measurements. First, liquid-based LSCs have been considered, in order to study the effects of self-absorption and to determine the optimal concentrations for fluorescent dyes. Once the optimal concentrations have been found, polymeric LSCs have been investigated with the same procedure, paying attention to the effects of the LSCs' size on its EQE. For single-layer LSC devices, EQE measurements are in good agreement with our theoretical model. LSCs doped with dye C show higher short-circuit current densities with respect to those doped with dye B, even if dye C has a lower fluorescence quantum yield with respect to other dyes. This is because absorption of dye C is shifted towards the red, where the solar photon flux is richer. This result suggests that new and improved fluorescent dyes have to be synthesized in order to absorb in the low energy visible and infrared spectral ranges. New organic dyes as well as inorganic compounds, like semiconductor quantum dots, are currently being investigated for this purpose.

Finally, it is evident that self-absorption, scattering losses and bulk absorption within the matrix represent severe limits for development of large-area LSCs. For this reason much attention will be devoted to the synthesis of new fluorescent dyes with a greater shift between absorption and emission, as well as in the production of high-quality, high transparency polymeric materials.

6 REFERENCES

[1] J.S. Batchelder, A.H. Zewail, and T. Cole, Appl. Opt. **18**, 3090 (1979); ibid. **20**, 3733 (1981).

[2] W.G.J.H.M. van Sark et al., Opt. Express **16**, 21773 (2008).

[3] L.H. Slooff et al., Phys. Status Solidi (RRL) **2**, 257 (2008).

[4] J.C. Goldschmidt et al., Solar Energy Materials & Solar Cells **93**, 176182 (2009).

[5] P.F. Scudo, L. Abbondanza, R. Fusco, and L. Caccianotti, Solar Energy Mat. Solar Cells 94, 1241 (2010).

[6] AM 1.5 solar spectrum irradiance data: http://rredc.nrel.gov/solar/spectra/am1.5/

[7] A. Alessi, R. Fusco, A. Proto, G. Schimperna, P. Scudo, Composizioni fotoluminescenti per convertitori di spettro a migliorata efficienza, Italian patent application number MI09A001796.

[8] S. Flores Daorta, M. Liscidini, L.C. Andreani, P. Scudo and R. Fusco in *Proceeding of the 26th European Photovoltaic Conference and Exhibition*, Session Reference 1CV.3.11, Abstract No. 1181, Hamburg (2011).